Nanoscale Res Lett (2010) 5:637–643
DOI 10.1007/s11671-010-9527-z

NANO EXPRESS

Ionic Transport Properties in Nanocrystalline $Ce_{0.8}A_{0.2}O_{2-\delta}$ (with A = Eu, Gd, Dy, and Ho) Materials

Ashok Kumar Baral · V. Sankaranarayanan

Received: 16 October 2009 / Accepted: 5 January 2010 / Published online: 30 January 2010

Abstract The ionic transport properties of nanocrystalline 20 mol% Eu, Gd, Dy, and Ho doped cerias, with average grain size of around 14 nm were studied by correlating electrical, dielectric properties, and various dynamic parameters. Gd-doped nanocrystalline ceria shows higher value of conductivity (i.e., 1.8×10^{-4} S cm^{-1} at 550°C) and a lower value of association energy of oxygen vacancies with trivalent dopants Gd^{3+} (i.e., 0.1 eV), compared to others. Mainly the lattice parameters and dielectric constants (ε_{∞}) are found to control the association energy of oxygen vacancies in these nanomaterials, which in turn resulted in the presence of grain and grain boundary conductivity in Gd- and Eu-doped cerias and only significant grain interior conductivity in Dy- and Ho-doped cerias.

Keywords Nanostructures · Electrical transport · Dielectric relaxations · Association energy

Introduction

The microcrystalline rare-earth-doped ceria-based materials are very good oxide ionic conductors at intermediate temperatures, and these materials have been considered as alternative of the yttria-stabilized zirconia as the electrolyte of the solid oxide fuel cell (SOFC) [1, 2]. Major problem associated with the ceria-based electrolytes is the reduction of Ce^{4+} to Ce^{3+} under reducing condition at temperatures above 700°C, resulting high electronic conductivity, which is detrimental to the function of electrolyte in the SOFCs [3]. However, it has been observed that the reduction for ceria-based materials can be neglected at temperatures below 700°C [4]. In order to use the ceria-based materials as electrolyte below 700°C, it is highly desirable to increase the ionic conductivity at lower temperatures. In the case of polycrystalline ceria-based electrolytes, the impurities such as Si and Ca segregate at grain boundaries and form thin blocking layers within the grain boundary network [5], which affect the grain boundary conductivity. It has been considered that, by reducing the grain size of the materials, total amount of impurities can be spread over a large interfacial area and the effect of impurities can be reduced. Hence, the grain boundary conductivity as well as overall ionic conductivity of the materials can be increased. It has been also speculated that the grain boundary may provide faster diffusion pathway for ionic defects resulting in enhanced ionic conductivity in the finely grained materials [6]. It is therefore expected that, by reducing the grain size of the ceria-based materials into nano scale, conductivity of the materials can be increased, and the materials can be used at lower temperatures to avoid the reduction of Ce^{4+} to Ce^{3+}, which leads to the electronic conductivity of the materials, so that it would be helpful in reducing the operating temperature of SOFC. Since the reduction of operating temperature of SOFC (which is expected to be the alternative energy source for future generation) has been a subject of interest world wide, recently a considerable interest has been increased on the development of nanostructured ceria-based electrolyte materials. Various synthesis and processing methods have been used to prepare the pure ceria or doped ceria nanocrystalline materials with desired properties. These include gel casting process [7], chemically processed method and IGC method [8], carbonate co-precipitation method [9] etc. Apart from nanoparticles, the doped or undoped cerias in

A. K. Baral (✉) · V. Sankaranarayanan
Department of Physics, Indian Institute of Technology Madras, Chennai 600036, India
e-mail: ashok@physics.iitm.ac.in

the form of nanotubes, nanorods, and nanowires are also being considered for useful application in fuel cells. The morphology controlled synthesis of various nanorods, nanotubes, and nanowires of ceria-based materials have been proposed by various authors elsewhere [10–13]. However, since the physical and chemical properties of these nanomaterials are synthesis process and grain size dependent, these properties are currently under debate and not yet clearly understood.

In this work, we have discussed the electrical and dielectric properties and their correlations in the nanostructured 20 mol % of Eu-, Gd-, Dy-, and Ho-doped ceria-based materials for in-depth understanding of ionic transport process in nano scale. A comparison study of various dynamic parameters has been carried out to have a clear idea of the fundamental reason behind the variation in association energy of oxygen vacancies in these nanostructured materials with dopants of different ionic radii and its effect on ionic conductivity of these nanostructured materials.

Experimental

The nanocrystalline materials of 20 mol% Eu-, Gd-, Dy-, and Ho-doped cerium oxide ($Ce_{0.8}A_{0.2}O_{2-\delta}$, A = Eu, Gd, Dy, and Ho) were prepared by citrate auto ignition method using CeO_2, Eu_2O_3, Gd_2O_3, Dy_2O_3, and Ho_2O_3 as starting materials, as described in our previous work on Ho-doped ceria [14]. The precursors obtained for different materials were calcined at 800°C for 5 h to get single phase nanocrystalline materials. The phase purity and crystal structures of calcined powders were studied by X-ray diffraction and high-resolution TEM. The ionic transference numbers of the nanocrystalline material in pellet form were calculated in air atmosphere using the Wagner's dc polarization technique as described by Baral and Sankaranarayanan [15], and these values are found to be around 85 at 500°C. The ac electrical and dielectric properties of materials (in pellet form) were studied using electrochemical impedance spectroscopy. The impedance measurements were carried out using two probe method in air, varying the temperature from 250 to 550°C and the frequency from 1 to 10 MHz. The silver paste was also used on both sides of pellets (sintered at 800 for 2 h each) as electrodes in the impedance measurement as well as dc polarization technique. The densities of the pellets of different materials used for both the experiments were between 93 and 95% of the theoretical density. Since the calcination temperature of powder materials and sintering temperature of the pellets were same, the average grain size in the sintered pellets are found to remain same and the nanocrystallinity in the pellets is maintained in the sintered pellets, as it was observed in our previous result [15].

Results and Discussion

Figure 1 shows the powder X-ray diffraction patterns of the Gd-, Eu-, Dy- and Ho-doped nanocrystalline cerias calcined at 800°C for 5 h and these materials are abbreviated here as GDC0.2, EuDC0.2, DyDC0.2, and HDC0.2, respectively. Comparing with the X-ray diffraction pattern of Ho-doped ceria, which has already been reported earlier [14], the Gd-, Eu- and Dy-doped cerias are also found to be in single-phased cubic fluorite structure. The average crystallite size of the materials were calculated by Debye-Sherrer formula and these are found to be 13, 12, 15, and 14 nm, respectively, for Gd-, Eu-, Dy- and Ho-doped nanocrystalline materials. So it is observed that the average crystallite sizes of these materials (with different dopants), calcined at same temperatures (i.e., 800°C), are almost same. The lattice parameters of the materials were calculated by the software "Celn" and these are found to be 5.429, 5.432, 5.425, and 5.389 Å, respectively, in case of the nanomaterials with Eu, Gd, Dy, and Ho as dopants, which indicate that there exists a lattice expansion as the ionic radius of dopant increases, except the ceria doped with Eu^{3+}. Even though Eu^{3+} has a bit larger ionic radius than that of Gd^{3+}, the nanocrystalline EuDC0.2 material shows a lower value of lattice constant than that of GDC0.2. Figure 2a and b show the high-resolution TEM micrographs of the Gd- and Eu-doped ceria, which indicate that the material particles are single crystalline in nature, with the lattice oriented in a single direction in every particles. The similar microstructures are also observed in the case of Dy- and Ho-doped ceria [14]. Since the particles are single crystalline in nature, the average crystallite sizes are considered as equal to the average grain sizes in respective materials.

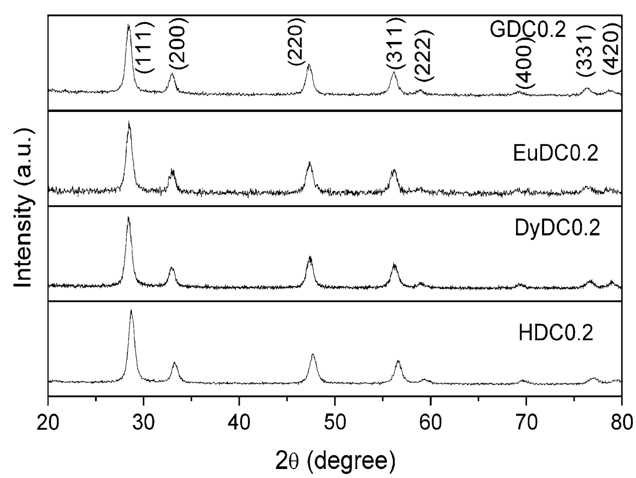

Fig. 1 The powder XRD patterns of nanocrystalline GDC0.2, EuDC0.2, DyDC0.2, and HDC0.2 materials calcined at 800°C for 5 h

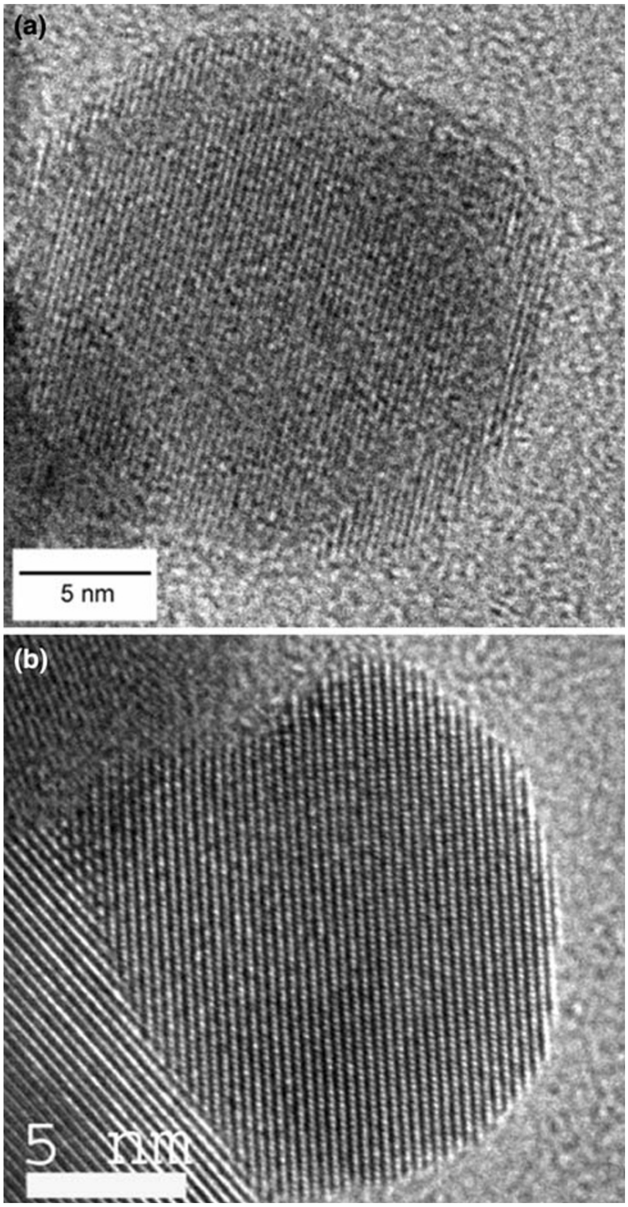

Fig. 2 **a** and **b** show the high-resolution TEM micrographs of GDC0.2 and EuDC0.2 materials, respectively. Sizes of the particles shown here are around 21 and 17 nm in case of (**a**) and (**b**), respectively

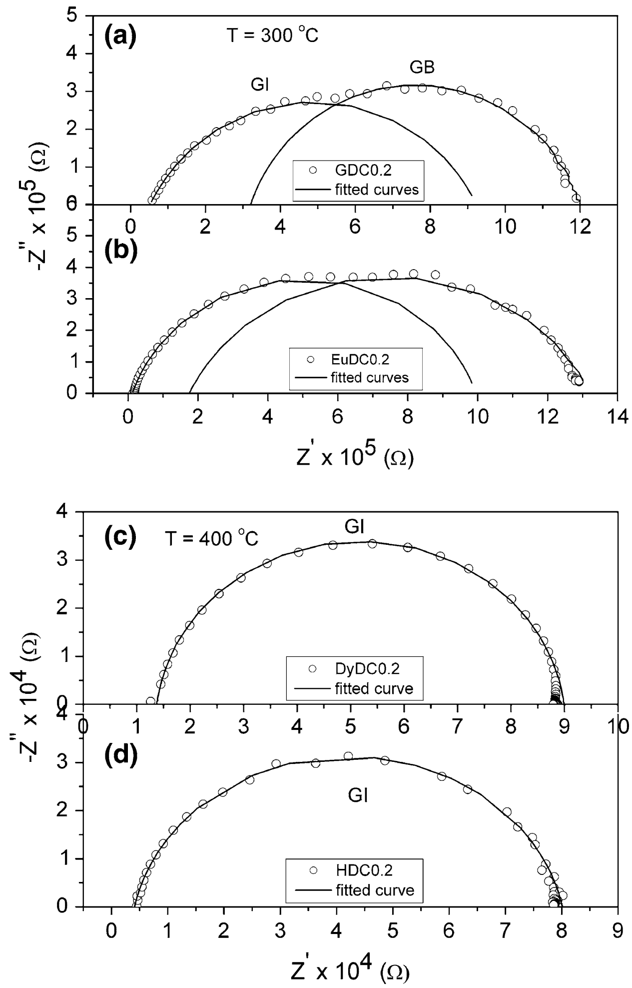

Fig. 3 **a** and **b** Complex impedance plots of the nanocrystalline GDC0.2 and EuDC0.2 at 300°C. GI and GB correspond to the grain interior and grain boundary, respectively; **c** and **d** are the complex impedance plots of DyDC0.2 and HDC0.2 at 400°C. Symbols are the obtained data points, and solid semicircles are the fitted data

Figure 3a–d show the complex impedance plots of the nanocrystalline GDC0.2, EuDC0.2, DyDC0.2, and HDC0.2 materials, respectively, at different temperatures. The plots show that in case of the materials GDC0.2 and EuDC0.2 both the grain and the grain boundary contribute to the total conductivity of the materials, whereas in case of DyDC0.2 and HDC0.2, the presence of grain interior conductivity is only observed, even though the grain boundary conductivity is expected in the nanomaterials. The similar conductivity properties of these materials are observed at all the temperatures. As the temperature increases, the conductivity of all the materials increases. Figure 4 shows the Arrhenius plots of the conductivity in different materials. The values of conductivities and activation energies are listed in the Table 1. The nanocrystalline GDC0.2 material shows the higher value of conductivity compared to other materials at all the temperatures.

Figure 5 shows the frequency spectra of conductivity of the materials at 400°C. As the conductivity of HDC0.2 [14] (which is also shown here for comparison), the conductivity spectra in case of GdDC0.2, EuDC0.2, and DyDC0.2 exhibit the behaviour of ionic materials with a dc plateau at lower frequencies followed by dispersion at higher frequency region. The observed conductivity behaviour agrees well with the prediction of Jump relaxation model [16, 17], which suggests that at lower frequencies an ion jumping from one site to its neighbouring vacant site successfully contributes to the dc conductivity. The

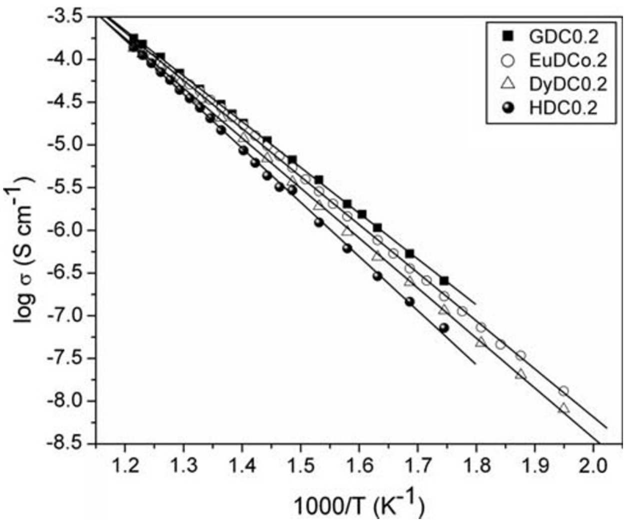

Fig. 4 Arrhenius plots of total conductivity in GDC0.2, EuDC0.2, DyDC0.2, and HDC0.2 materials in the temperature range 250–550°C

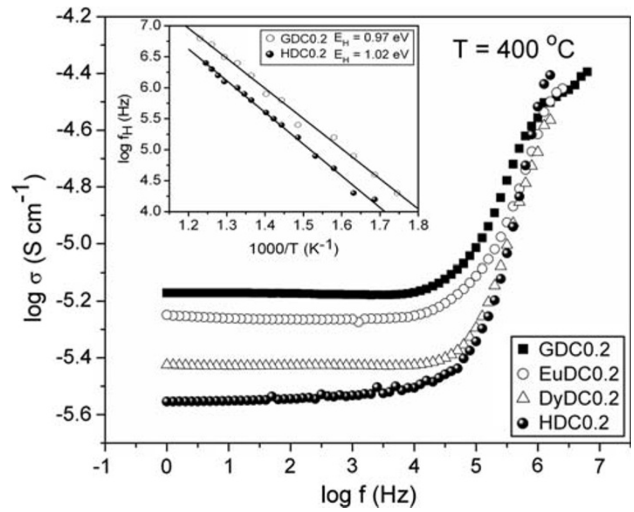

Fig. 5 Plots of ac conductivity as a function of frequencies at 400°C, in the case of GDC0.2, EuDC0.2, DyDC0.2, and HDC0.2 materials. Inset shows the Arrhenius plots of hopping frequency i.e., log f_H versus 1/T in case of GDC0.2 and HDC0.2

electrical conduction takes place in these nanocrystalline materials through hopping, and the correlated forward–backward hopping together with relaxation of ions gives rise to conductivity dispersion at higher frequencies. The characteristic hopping frequency is identified as the frequency at which $\sigma = 2\sigma_{dc}$ [18], where σ_{dc} is the dc conductivity and it is obtained from the conductivity value at zero frequency limit in the Fig. 5. The hopping frequencies are found to be temperature dependent and obey the Arrhenius relation: $f_H = f_o \exp(-E_H/K_BT)$, where f_o is the pre-exponential factor of hopping frequency, and E_H is the activation energy for the hopping. From the Arrhenius plots shown in inset of Fig. 5, the hopping activation energy (E_H) of charge carriers are found to be 0.97, 0.76, 0.92, and 1.02 eV in case of GDC0.2, EuDC0.2, DyDC0.2, and HDC0.2, respectively.

Figure 6 shows the variation of dielectric constant (ε') with frequency in case of the nanocrystalline GDC0.2, EuDC0.2, and DyDC0.2 materials at 400°C. The plots exhibit sharp upturn and high values of ε' at lower frequencies due to the polarization of charge carriers at the electrode–electrolyte interface [19], as observed in HDC0.2 [14]. With increase in temperature, the polarization also increases due to the enhancement of mobility of charge carriers in all the materials. The values of dielectric constant ε_∞ (the high frequency limit of ε') of materials at different temperatures are listed out in the Table 2.

Figure 7 shows the frequency spectra of electric modulus M″ at 300°C in case of GDC0.2, EuDC0.2, and DyDC0.2 materials. It is observed that at lower temperatures, the modulus spectra consist of a relaxation peak in case of all the materials. The peaks in the Fig. 7 can be attributed to the relaxation reorientation of defect associates (Eu-$V_o^{\bullet\bullet}$)$^\bullet$ and (Dy-$V_o^{\bullet\bullet}$)$^\bullet$ present in the EuDC0.2 and DyDC0.2 materials, respectively, as observed in HDC0.2 material [14] as well as in the case of nanocrystalline 15 mol % Gd-doped ceria [15] and microcrystalline La-doped ceria [20]. This is because when trivalent cations (say) A^{3+} are doped in cubic fluorite structured ceria, one oxygen vacancy is created in the lattice for every two trivalent cations (A^{3+}), and the oxygen vacancy associates with one of the A^{3+} leaving the other one unpaired. In the association (A-$V_o^{\bullet\bullet}$)$^\bullet$ case, the $V_o^{\bullet\bullet}$ can occupy any of the eight equivalent sites around A^{3+} in cubic fluorite structure and jumps from one site to the other giving rise to the reorientation relaxation process. In other words, the motion of oxygen vacancy in this reorientation process is said to be

Table 1 Values of conductivity and activation energies in different materials

Materials	E_σ (eV)	σ_{gi} (S cm^{-1}) (at 550°C)	σ_{gb} (S cm^{-1}) (at 550°C)	σ (S cm^{-1}) (550°C)
GDC0.2	1.07	5.8×10^{-4}	7.3×10^{-4}	1.8×10^{-4}
EuDC0.2	0.91 (480–550°C)	3.45×10^{-4}	4.4×10^{-4}	1.39×10^{-4}
	1.13 (250–470°C)			
DyDC0.2	1.16			1.36×10^{-4}
HDC0.2	1.26			1.4×10^{-4}

E_σ is the total activation energy, whereas σ, σ_{gi}, and σ_{gb} are the total conductivity, grain interior conductivity and grain boundary conductivity, respectively

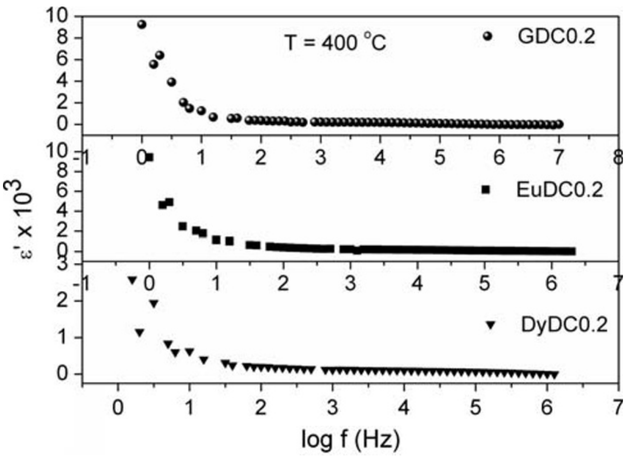

Fig. 6 Variation of real part of permittivity (ε') with frequency at 400°C, in the case of GDC0.2, EuDC0.2, and DyDC0.2 materials

Table 2 The values of dielectric constants (ε_∞) of the materials at different temperatures

Materials	ε_∞ (at 300°C)	ε_∞ (at 400°C)	ε_∞ (at 500°C)	ε_∞ (at 550°C)
GDC0.2	5.44	12.29	16.74	20.05
EuDC0.2	6.09	7.91	13.12	19.64
DyDC0.2	0.86	1.87	2.81	5.07
HDC0.2	4.46	4.73	11.28	17.68

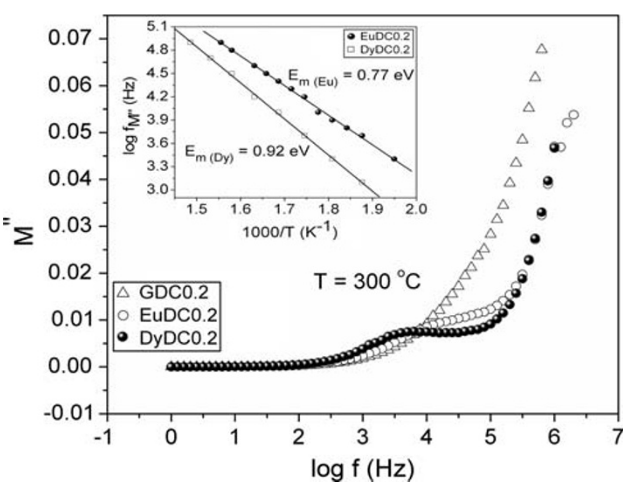

Fig. 7 Frequency spectra of electric modulus M″ at 300°C in case of GDC0.2, EuDC0.2, and DyDC0.2 materials. Inset shows the Arrhenius plots of peak frequencies ($f_{M''}$) in case of the EuDC0.2 and DyDC0.2 materials

a bound motion i.e., the oxygen vacancy $V_o^{\bullet\bullet}$ remains bound to A^{3+} and jump between the nearest neighbour positions of the cations (A^{3+}) in all the materials. With increase in temperature, the peak shifts towards the higher frequencies. The activation energy for reorientation of oxygen vacancy is obtained from the Arrhenius plot of peak frequencies ($f_{M''}$) in different materials as shown in inset of Fig. 7 and these values are found to be 0.77 and 0.92 eV, respectively in EuDC0.2 and DyDC0.2, whereas in our previous result on HDC0.2, it is found to be 1.02 eV [14].

Generally, the activation energy for the bound motion is considered as the migration energy of free vacancy ($V_o^{\bullet\bullet}$) in the long range motion [20]. The total activation energy (E_σ) being the sum of the association energy (E_{asso}) and migration energy (E_m), the association energies in EuDC0.2 is found to be 0.14 eV ($E_{asso(Eu)} = 0.91$–0.77 eV). Similarly, in case of DyDC0.2, it is 0.24 eV (since $E_{asso(Dy)} = 1.16$–0.92 eV), and in the case of HDC0.2 material, the value of association energy is found to be 0.24 eV [14]. It is observed that in case of EuDC0.2 and DyDC0.2 materials, the migration energy (E_m) of oxygen ions in the long-range motion calculated from the dielectric relaxation peaks, match well with the activation energies (E_H) for hopping of charge carriers, as in case of HDC0.2 [14]. Hence, these values also support that in these nanomaterials, the migration of oxygen ions takes place through hopping, which was predicted earlier with respect to the behaviour of frequency spectra of conductivity. However, in the case of GDC0.2, the M″ spectra do not show any peak above 300°C, except at few lower temperatures. So it was difficult to find out the migration energy of oxygen vacancies from modulus spectra. Since the value of hopping energy is same as the migration energy of oxygen vacancies, as observed in the case of Eu-, Dy- and Ho-doped materials, the migration energy of the oxygen vacancies in the material GDC0.2 can be taken as 0.97 eV. Hence, the association energy in the GDC0.2 must be 0.1 eV (i.e., $E_{asso(Gd)} = 1.07 - 0.97$ eV).

It is observed from the Table 2 that the values of dielectric constant (ε_∞) of the nanocrystalline HDC0.2 are comparatively lower than that of EuDC0.2 and GDC0.2, at all the temperatures. On the other hand, the X-ray diffraction study indicates that there is a lattice contraction in this nanocrystalline Ho-doped ceria, and it is expected that the lattice contraction might have resulted in a smaller value of inter ionic separation between the oxygen vacancy and the trivalent dopant Ho^{3+}. Since the values of both the dielectric constant (ε_∞) and the inter ionic distance (r) are smaller, the value of columbic interaction energy between the oxygen vacancy and the trivalent dopant Ho^{3+} i.e.,

$$E = \left|\frac{-2e^2}{4\pi\varepsilon_0\varepsilon_r r^2}\right| \quad (1)$$

(where r is the distance between the oxygen vacancy and its associated Ho^{3+}, and ε_r is the dielectric constant) [15], must be higher. This could be the reason for the high value of association energy (i.e., 24 eV) between the oxygen vacancy and its associated Ho^{3+}, in the nanocrystalline HDC0.2 material.

Similarly, based on values of lattice constants, the inter ionic spacing (r) in the case of material DyDC0.2 can be expected to be smaller compared to that of EuDC0.2 and GDC0.2, even though it must be larger than the value of "r" in HDC0.2. The values of dielectric constant ε_∞ of the material DyDC0.2 are also found to be mush lower than that of others, at all the temperatures. This must be the reason for high value of the columbic interaction energy between the oxygen vacancy ($V_o^{\bullet\bullet}$) and the trivalent dopant Dy^{3+}, which results in a high value of association energy (0.24 eV) in the nanocrystalline DyDC0.2 material, as in case of HDC0.2. Since in the case materials HDC0.2 and DyDC0.2, the oxygen vacancies are strongly associated with trivalent dopant ions, it is expected that the local motion of oxygen vacancies around the dopants in side the grains mainly contributes to the conductivity of the materials, and hence this leads to the presence of only the grain interior conduction as shown in complex impedance plots of DyDC0.2 and HDC0.2 materials (Fig. 3c, d).

However, in the case of GDC0.2 and EyDC0.2, the values of dielectric constants are comparatively higher and since the lattice constants are comparatively larger, the inter ionic distances must be larger compared to that of DyDC0.2 and HDC0.2. This could be the reason of lower values of association energies (i.e., 0.1 and 0.14 eV, respectively) in the materials GDC0.2 and EuDC0.2 compared to that of DyDC0.2 and HDC0.2. Even, comparing the materials GDC0.2 and EuDC0.2, the values of dielectric constant of GDC0.2 is higher than that of EuDC0.2 as shown in Table 2 and of course the value of "r" can expected to be larger in GDC0.2 than that in the case of EuDC0.2. This clearly indicates that the columbic interaction energy must be lower in GDC0.2. Therefore, association energy in GDC0.2 (i.e., 0.1 eV) is lower compared to that in case of EuDC0.2 (i.e., 0.14 eV).

The values of association energy in the nanocrystalline GDC0.2 and EuDC0.2 materials being much smaller (than that of DyDC0.2 and HDC0.2), the oxygen vacancies must be free at higher temperatures. Generally, at higher temperatures, the concentration of free oxygen vacancy is expected to be more at grain boundary regions, which results in the significant grain boundary conduction in both the GDC0.2 and EuDC0.2 materials, as shown in their complex impedance plots (Fig. 3a, b). However, the migration energy (E_m) of free oxygen vacancies being comparatively smaller (i.e., 0.77 eV) in EuDC0.2 than that of others, there must be an easy migration of free oxygen vacancies in the grain boundary regions at higher temperatures. This resulted in a bend in the Arrhenius plot of conductivity (shown in Fig. 4) of EuDC0.2, with a lower value of total activation energy (i.e. 0.91 eV) above 470°C.

Comparing with our previous results on 15 mol% Gd-doped ceria [15], the present GDC0.2 material has larger lattice constant and hence inter ionic separation between them must be larger compared to that in GDC0.15. So this should have resulted in lower association energy in GDC0.2. But much higher value of dielectric constant (ε_∞) of GDC0.15 compared to that of GDC0.2 resulted in a lower value of the association energy in GDC0.15 (i.e., 0.07 eV). So, from these results it can be predicted that the values of lattice constants and dielectric constants play major roles in controlling the association energy in these nanostructured rare-earth-doped cerias.

Conclusion

The electrical and dielectric properties of nanocrystalline 20 mol % Gd-, Eu-, Dy-, and Ho-doped ceria have been thoroughly studied. Various dynamic parameters such as lattice constants, conductivity, hopping energy, dielectric constants, migration energies, association energy are obtained in the intermediate temperature range and compared. All the materials show good range of ionic conductivity for the potential application, in intermediate temperature region. Gd-and Eu-doped ceria exhibited the presence of both grain interior and grain boundary conductivity, whereas in the case of Dy- and Ho-doped materials, the grain interior conductivity is only observed. GDC0.2 shows high value conductivity and low value of association energy compared to others as observed in microcrystalline materials. Oxygen ions follow the hopping mechanism during conduction in all the nanostructured materials. Comparing with present and reported results, it is observed that the values of lattice constants and dielectric constants mainly control the association energy of oxygen vacancies, which in turn decides the presence of both grain and grain boundary conductivities or only the grain interior conductivity in these nanostructured rare-earth-doped cerias.

References

1. B.C.H. Steele, T. Takahashi, *High Conductivity Solid Ionic Conductors* (World Scientific, Singapore, 1989)
2. H. Inaba, H. Tagawa, Solid State Ionics **83**, 1 (1996)
3. M. Mogensen, N.M. Sammes, G.A. Tompsett, Solid State Ionics **129**, 63 (2000)

4. S.J. Hong, K. Meheta, A.V. Viarkar, J. Electrochem. Soc. **145**, 638 (1998)
5. R. Gerhardt, A.S. Nowick, J. Am. Ceram. Soc. **69**, 641 (1986)
6. D. Vaben, D. Stover, L.G.J. de Haart, M. Cappadonia, Br. Ceram. Proc. **56**, 35 (1996)
7. J.G. Cheng, S.W. Zha, J. Huang, X.Q. Liu, G.Y. Meng, Mater. Chem. Phys. **78**, 791 (2003)
8. Y.M. Chiang, E.B. Lavik, I. Kosacki, H.L. Tuller, J. Electroceram. **1**, 7 (1997)
9. T.S. Zhang, J. Ma, L.H. Luo, S.H. Chan, J. Alloys Comp. **422**, 46 (2006)
10. Y. Fu, Z.D. Wei, M.B. Ji, L. Li, P.K. Shen, J. Zhang, Nanoscale Res. Lett. **3**, 431 (2008)
11. D. Zhang, H.X. Fu, L.Y. Shi, C.S. Pan, Q. Li, Y.L. Chu, W. Yu, Inorg. Chem. **46**, 2446 (2007)
12. C. Sun, H. Li, Z.X. Wang, L. Chen, X. Huang, Chem. Lett. **33**, 662 (2004)
13. K. Zhou, Z. Yang, S. Yang, Chem. Mater. **19**, 1215 (2007)
14. A.K. Baral, V. Sankaranarayanan, Physica B **404**, 1674 (2009)
15. A.K. Baral, V. Sankaranarayanan, Appl. Phys. A Mater. Sci. Process. **98**, 367 (2010)
16. K. Funke, Solid State Ionics **94**, 27 (1997)
17. J.C. Dyre, J. Appl. Phys. **64**, 2456 (1988)
18. D.P. Almond, A.R. West, Solid State Ionics **9–10**, 277 (1983)
19. L.M. Hodge, M.D. Ingram, A.R. West, J. Electroanal. Chem. **74**, 25 (1976)
20. P. Sarkar, P.S. Nicholson, J. Am. Ceram. Soc. **72**, 1447 (1989)